JOURNAL OF Materials CHEMISTRY

Intermolecular organisation of triphenylene-based discotic mesogens by interdigitation of alkyl chains†

Matthew T. Allen,[a] Siegmar Diele,[b] Kenneth D. M. Harris,*[a] Torsten Hegmann,[c] Benson M. Kariuki,[b] Dirk Lose,[b] Jon A. Preece*[a] and Carsten Tschierske[c]

[a]*School of Chemistry, The University of Birmingham, Edgbaston, Birmingham, UK B15 2TT. E-mail: K.D.M.Harris@bham.ac.uk, J.A.Preece@bham.ac.uk*
[b]*Institute of Physical Chemistry, Martin-Luther-University Halle, Mühlpforte 1, D-06118 Halle, Germany*
[c]*Institute of Organic Chemistry, Martin-Luther-University Halle, Kurt-Mothes-Strasse 2, D-06120 Halle, Germany*

Received 24th August 2000, Accepted 11th October 2000
First published as an Advance Article on the web 1st December 2000

Two series of hexakis(alkyloxy)triphenylenes have been synthesised and characterised. All materials contain two different lengths of *n*-alkyloxy chains. *Series I* (**C_mC_n**) materials contain three $-OC_5H_{11}$ chains and three $-OC_nH_{2n+1}$ chains. *Series II* (**C_mC_n**) materials contain three $-OC_mH_{2m+1}$ chains and three $-OC_nH_{2n+1}$ chains, such that $m+n=10$. Hexagonal columnar mesophases are observed in *Series I* for $n \geqslant 3$ and, in *Series II*, for **C_5C_5** and **C_6C_4**. Investigation by XRD shows that, within *Series I*, increasing the C_n chain length increases the intercolumnar spacing. Furthermore, the intercolumnar spacings for constitutional isomers are identical. The difference in the lengths of the two types of alkyl chain at the periphery of the molecules is defined as the Interdigitation Length (IL) and is a measure of the maximum extent of interdigitation that is possible between neighbouring molecules. *Series I* and *II* materials have been studied to probe the effect of IL on the change in enthalpy (ΔH_{Col-I}) and entropy (ΔS_{Col-I}) for the mesophase to isotropic liquid phase transition. In contrast to **C_xC_x** materials, which show a decrease in ΔH_{Col-I} and ΔS_{Col-I} with increasing chain length, *Series I* and *II* mesogens all exhibit ΔH_{Col-I} and ΔS_{Col-I} values similar to those of long chain **C_xC_x** materials, irrespective of chain length.

1. Introduction

Since their discovery in 1977 by Chandrasekhar,[1] discotic mesogens have been of great interest to the liquid crystal community. The first discotic liquid crystal was a hexa-substituted benzene derivative[1] and now there is a wide range of discotic cores, including, for example, triphenylene,[2,3] phthalocyanine[4] and pyrene[5] derivatives. Discotic molecules can form a variety of mesophases. The least ordered phase is the nematic discotic (N_d),[6,7] in which the molecular directors are aligned but with a random distribution of the molecules parallel to this director. More ordered phases are the hexagonal columnar (Col_h),[8–12] rectangular columnar (Col_r)[13] and oblique columnar (Col_{ob})[14] phases.

Many potential applications for discotic mesogens aim to exploit the phenomenon of photoconductivity,[15] in which electrons are excited to conduction bands yielding a photocurrent.[16] Photoconductivity has been observed in inorganic materials[16] such as crystalline and amorphous silicon, selenium–tellurium alloys, cadmium sulfide and zinc oxide. Silicon, for example, exhibits charge mobilities in the range of 0.5–1.5×10^3 $cm^3\ V^{-1}\ s^{-1}$. Examples of organic materials that exhibit photoconductivity include crystalline anthracene[16–20] and the charge-transfer complex of poly(vinylcarbazole) and trinitrofluorenone (PVK : TNF).[21]

Liquid crystalline materials have been shown to exhibit photoconductive properties.[8] For example, hexakis(alkyloxy)-triphenylenes form the Col_h mesophase[22] and have been shown to exhibit photoconduction.[8] Charge mobilities for hexakis(-pentyloxy)triphenylene are in the region of 10^{-3} $cm^2\ V^{-1}\ s^{-1}$ (see ref. 23). In contrast, hexakis(hexylthio)triphenylene forms a helical Col_h phase, which provides increased order of the mesophase[24] and a charge mobility of 0.1 $cm^2\ V^{-1}\ s^{-1}$ is observed, the highest charge mobility for a triphenylene-based photoconducting system (for comparison, we note that several one-dimensional organic metals are known,[25–27] the prototypical material of which is the co-crystal formed between tetrathiafulvalene and tetracyano-*p*-quinodimethane (TTF : TCNQ), which exhibits a charge mobility of 1 $cm^2\ V^{-1}\ s^{-1}$ and a conductivity of $5 \times 10^2\ \Omega^{-1}\ cm^{-1}$ (*cf.* Si which has a conductivity of $1 \times 10^{-3}\ \Omega^{-1}\ cm^{-1}$)[16]). An important aspect in using liquid crystalline materials as the basis of photoconductive systems is the fact that, on aligning the mesophase due to an external stimulus, the grain boundary defects (which trap charge in crystalline samples) do not exist. The liquid nature of the mesophase allows for a self-repair[16] mechanism and also provides good contact to the surface of metals, which is essential for device applications.

In view of the fact that increased charge mobilities appear to be associated with increased ordering of the columnar mesophases, the thrust of much research on triphenylene-based liquid crystals has been to introduce chemical modifications designed to increase the columnar ordering in terms of the average length of ordered stacking arrays along the column. Many examples of structural variations based on the simple hexakis(alkyloxy)triphenylenes[8–12] have been reported, including hexakis(alkylthio)triphenylenes,[28,29] polymer systems[30–33] and triphenylene oligomer formation,[34,35] as well as halogenation[36] and nitration[37,38] of the aromatic core. However, none of

†X-Ray diffraction data, quantities of reagents used in the syntheses and spectroscopic data for C_5C_n compounds are available as supplementary data. For direct electronic access see http://www.rsc.org/suppdata/jm/b0/b006916g/

 DOI: 10.1039/b006916g

these chemical modifications has led to an increase in the columnar ordering with a commensurate increase in photoconductivity. Recently, some of us have studied the adhesive forces generated by the interdigitation of alkyl chains[39] using atomic force microscopy. It was shown that by tailoring the interdigitating alkyl chains, the adhesive force between two surfaces could be controlled. Clearly it may be possible to use the idea of interdigitation of alkyl chains to influence the ordering in the hexagonal columnar mesophase of hexakis(alkyloxy)triphenylene liquid crystals. In this regard, the aim of the work described in the present paper has been to design and prepare appropriately derivatized hexakis(alkyloxy)triphenylenes such that the alkyl chains in one column interdigitate into the alkyl chain region of a neighbouring column.

In order to design an interdigitated system, at least two different chain lengths are required,[40–44] alternating around the triphenylene core (Fig. 1) and leading to an idealised network of molecules interlinked in a cog-like fashion (Fig. 2).

Here we report the first synthesis of two systematic series of such molecules, *Series I* and *Series II*[45] (Fig. 1), together with characterisation of their structural and thermal properties using polarized optical microscopy (POM), differential scanning calorimetry (DSC) and X-ray diffraction (XRD). The two series differ in the selection of the two types of alkyl groups at the periphery: C_mH_{2m+1} and C_nH_{2n+1}. In the notation adopted here, $\mathbf{C_mC_n}$ refers to a triphenylene molecule containing C_mH_{2m+1} and C_nH_{2n+1} alkyl chains. *Series I* materials contain three C_mH_{2m+1} ($m=5$) chains and three C_nH_{2n+1} chains ($n=1$–9), whereas *Series II* materials contain three C_mH_{2m+1} chains ($m=5$–8) and three C_nH_{2n+1} ($n=10$–m) chains. For comparison, we note that hexakis(alkyloxy)triphenylenes, which contain six C_xH_{2x+1} alkyl chains ($\mathbf{C_xC_x}$ in the notation adopted here), exhibit Col_h mesophases for $x \geqslant 4$. It may be envisaged that the mesophases of *Series I* and *II* materials may also display Col_h mesophases. Furthermore, the synthetic route adopted allows for the production of a $\mathbf{C_mC_n}$ molecule with C_3 symmetry (denoted by the suffix '**.sym**', *e.g.* $\mathbf{C_mC_n}$**.sym**) and an asymmetric isomer (denoted by '**.asym**', *e.g.* $\mathbf{C_mC_n}$**.asym**), Scheme 1. The difference between the alkyl chain lengths in a molecule $\mathbf{C_mC_n}$ ($|\boldsymbol{m}-\boldsymbol{n}|$) is called the Interdigitation Length (IL) and is a measure of the extent to which two molecules may interpenetrate each other through interdigitation. In summary, *Series I* provides a family of materials with an increasing number of alkyl carbon atoms per molecule. *Series II* provides a range of constitutional isomers, with varying interdigitation lengths.

For $\mathbf{C_xC_x}$ triphenylenes, a space filling model shows that the

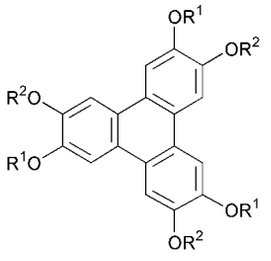

Series I $\mathbf{C_mC_n}$**.sym**
$R^1 = C_mH_{2m+1}$ (m = 5)
$R^2 = C_nH_{2n+1}$ (n = 1 - 9)

Series II $\mathbf{C_mC_n}$**.sym** ($m + n$ = 10)
$R^1 = C_mH_{2m+1}$, (m = 5 - 8)
$R^2 = C_nH_{2n+1}$, (n = 10 - m)

Fig. 1 Molecular structures of *Series I* and *Series II* materials: *Series I*:$\mathbf{C_mC_n}$ ($m=5$, $n=1$–9); *Series II:* $\mathbf{C_mC_n}$ ($m=5$–8, $n=10-m$; such that $m+n=10$).

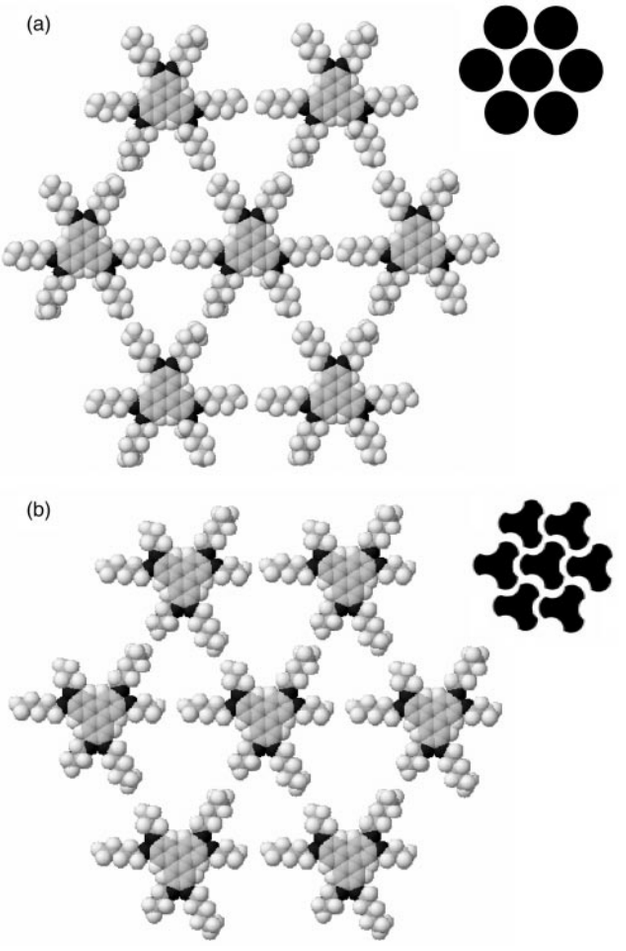

Fig. 2 Idealised packing of triphenylenes in the Col_h mesophase: (a) non-interdigitated $\mathbf{C_5C_5}$; (b) interdigitated $\mathbf{C_5C_3}$**.sym**.

mesophase packing object can be approximated by a disc (Fig. 2a). Clearly the *Series I* and *II* materials represent a modification of this disc, with protrusions in the region of the longer alkyl chains and voids in the region of the shorter alkyl chains, and the packing object thus resembles a propeller (Fig. 2b). In order to establish efficient packing, the protrusions of one molecule should be directed towards the voids of its neighbours (Fig. 2b). In effect, the short chains of one molecule should be close to the longer chains of its neighbours, thus interdigitating the alkyl regions of the two molecules. The potential for interdigitation varies both within *Series I* (for example, for $\mathbf{C_5C_3}$ IL = 2, for $\mathbf{C_5C_5}$ IL = 0 and for $\mathbf{C_5C_9}$ IL = 4) and *Series II* (IL increases from 0 ($\mathbf{C_5C_5}$), to 6 ($\mathbf{C_8C_2}$)).

Clearly the formation of interdigitated arrays of triphenylenes may be expected to affect the mobility and packing of the molecules within the mesophase in terms of intracolumnar ordering (Fig. 3a), intercolumnar lateral slippage (Fig. 3b) and rotational motion (Fig. 3c), which may depend significantly on the intercolumnar interactions.

In this regard, we may define two contrasting effects arising as a result of interdigitation:

(1) As the extent of interdigitation determines the extent of interlocking of molecules in neighbouring columns, interdigitation may promote the lateral slippage of molecules from column to column (Fig. 3b), and may therefore *decrease* the stability of the mesophase.

(2) Interdigitation may be expected to hinder the rotational mobility of the molecules (Fig. 3c), which may lead to an increase in the intracolumnar π–π interactions, and may therefore *increase* the stability of the mesophase.

Depending on the balance of these competing factors,

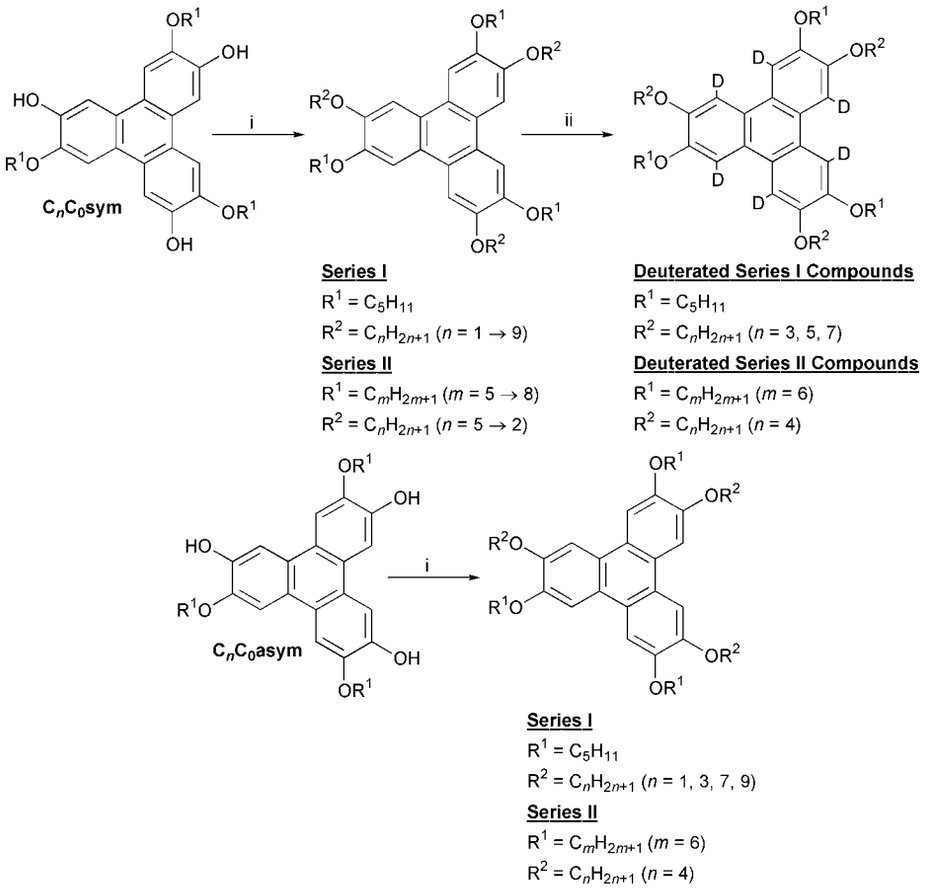

Scheme 1 General procedure for the synthesis of *Series I* and *Series II* compounds: the trihydroxytris(alkyloxy)triphenylenes were synthesized following preparations described in the literature.[46–49] i, R^1Br, K_2CO_3, CH_3CN, 82 °C, 20 h.; ii, D_2SO_4, D_2O, MeOD, 80 °C, 30 h.

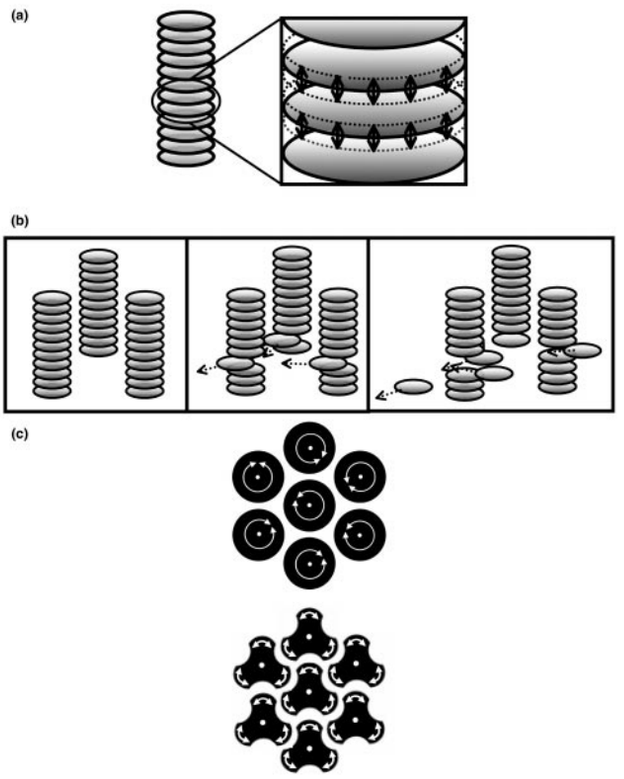

Fig. 3 (a) Intracolumnar molecular motion. (b) An illustration of the concept of intercolumnar 'slippage'. (c) An example of the difference in packing of D_{3h} and C_{3h} symmetry objects in a triangular array and the effect on axial rotation.

interdigitation of the alkyl chains may be expected either to increase or decrease the mesophase order. Thus, within a series of molecules with increasing IL, the mesophase order may vary in a non-linear fashion, depending on the relative contributions of these competing factors for each member of the series.

2. Results and discussion

2.1. Synthesis

The two series of triphenylene-based mesogens are illustrated in Fig. 1.

Series I materials comprise the triphenylene core, surrounded by two different *n*-alkyloxy chains, $-OR^1$ and $-OR^2$.

In *Series I*, $R^1 = C_mH_{2m+1}$ ($m = 5$) and $R^2 = C_nH_{2n+1}$ ($n = 1$–9). *Series II* materials again contain six *n*-alkyloxy chains: $R^1 = C_mH_{2m+1}$ ($m = 5$–8) and $R^2 = C_nH_{2n+1}$ ($n = 10$–m) such that $m + n = 10$. *Series I* compounds were synthesised following the general synthetic route shown in Scheme 1. Catechol was alkylated with 1-bromopentane as described in the literature.[46] Hexakis(pentyloxy)triphenylene, **C_5C_5** (D_{3h} point group), was prepared by the trimerisation of 1,2-bis(pentyloxy)benzene as described in the literature, using both the ferric chloride[46] route and molybdenum pentachloride[47] route. The formation of the two trihydroxy constitutional isomers (Scheme 1), **C_5C_0.sym** (C_{3h} point group) and **C_5C_0.asym** (C_s point group), was achieved using 9-bromobicycloborononane, 9-Br-BBN,[48] to effect the selective tris-dealkylation. The two isomers were separated by silica gel chromatography, allowing subsequent alkylation of **C_5C_0.sym** and **C_5C_0.asym** to yield the constitutionally pure compounds **C_5C_n.sym** and **C_5C_n.asym**. *Series II* compounds were synthesised in a similar manner to *Series I* compounds, and the general procedure is shown in Scheme 1. Trimerisation of the 1,2-bis(alkyloxy)benzene was achieved,

using either ferric chloride[46] or molybdenum pentachloride[47] and the hexakis(alkyoxy)triphenylene was dealkylated using either 9-Br-BBN[48] or *B*-bromocatecholborane,[49] to afford the trihydroxy constitutional isomers $\mathbf{C_mC_0}$**.sym** and $\mathbf{C_mC_0}$**.asym**. Separation of these isomers was achieved by silica gel chromatography and the subsequent re-alkylation yielded the constitutional isomers $\mathbf{C_mC_n}$**.sym** and $\mathbf{C_mC_n}$**.asym**.

Aromatic deuteration of triphenylene materials has been carried out for the purposes of investigating mesophase motion by ^{2}H NMR. The triphenylene material was refluxed for 72 hours in a mixture of D_2SO_4, D_2O and MeOD. The degree of deuteration, analysed by mass spectrometry, showed that, on average, five to six aromatic protons had been exchanged for deuterium.

2.2. *Series I*

2.2.1. Optical characterisation. POM studies show that the *Series I* materials exhibit a mesophase for $n = 3$–9. These materials display characteristic defect textures for the columnar hexagonal (Col_h) mesophase, examples of which are shown in Fig. 4 for $\mathbf{C_5C_3}$**.sym**, $\mathbf{C_5C_7}$**.sym** and $\mathbf{C_5C_9}$**.sym**. The materials $\mathbf{C_5C_1}$**.sym** and $\mathbf{C_5C_2}$**.sym** do not exhibit transitions to mesophases.

2.2.2. X-Ray diffraction analysis. Structural analysis in the mesophases by X-ray diffraction has been carried out using photographic and, for $\mathbf{C_5C_3}$**.sym** and $\mathbf{C_5C_9}$**.sym**, diffractometric methods.

The X-ray diffraction photographs (Fig. S1 in Supplementary Information) confirm the formation of a Col_h mesophase for the materials from $\mathbf{C_5C_3}$**.sym** to $\mathbf{C_5C_9}$**.sym**. From the X-ray diffraction photographs (Fig. S1 in Supplementary Information) the intercolumnar spacings for each material can be determined. The *d*-spacing (denoted d_{100}) of the intense, sharp (100) peak at low diffraction angles gives the perpendicular distance between adjacent lattice planes (Fig. 5). The intercolumnar spacing for a hexagonal lattice is obtained by division of d_{100} by ($\cos 30^\circ$). For the members of *Series I* that form mesophases, there is a monotonic increase in the intercolumnar spacing as *n* increases, as illustrated in Fig. 6a and 6b. The increasing intercolumnar spacing is expected on the basis of the interdigitation model (Fig. 2), as the total alkyl chain length for the shorter and longer chains increases from 8 carbon atoms ($\mathbf{C_5C_3}$**.sym**) to 14 carbon atoms ($\mathbf{C_5C_9}$**.sym**) within *Series I* and, assuming that the densities of the materials in their mesophases are similar, should give rise to an increasing intercolumnar spacing (Fig. 6a and 6b). Note that the densities of all *Series I* and *II* materials, estimated from the unit cell volumes, are close to 1 g cm^{-3} (Fig. 6a), with evidence for a small odd–even effect. Comparison of the intercolumnar spacings for constitutional isomers of the *Series I* materials and for the corresponding $\mathbf{C_xC_x}$ materials ($\mathbf{C_4C_4}$[8] and $\mathbf{C_7C_7}$[50] plotted in Fig. 6b) show very similar intercolumnar spacings for $\mathbf{C_5C_3}$**.sym** and $\mathbf{C_4C_4}$ (18.5 Å) and for $\mathbf{C_5C_9}$**.sym** and $\mathbf{C_7C_7}$ (22.2 Å and 22.6 Å respectively). This observation is consistent with the interdigitation packing model being adopted in the mesophases of the *Series I* materials.

For $\mathbf{C_xC_x}$ discotic compounds, it is not common to observe the (210) reflection for the mesophase, with the exception of $\mathbf{C_4C_4}$, which displays several reflections in the mesophase.[51] However, the (210) reflection is observed for the following $\mathbf{C_5C_n}$ materials in *Series I* (Fig. S2 in Supplementary Information): $\mathbf{C_5C_3}$**.sym**, $\mathbf{C_5C_4}$**.sym**, $\mathbf{C_5C_7}$**.sym** and $\mathbf{C_5C_9}$**.sym**. Furthermore, $\mathbf{C_5C_3}$**.sym** also exhibits the (200) reflection (Fig. S2 in Supplementary Information).

The X-ray diffraction photographs for the mesophases (Fig. S1 in Supplementary Information) also provide information about the intermolecular spacing within a column and thus gives information on the nature of the π–π stacking. The broad

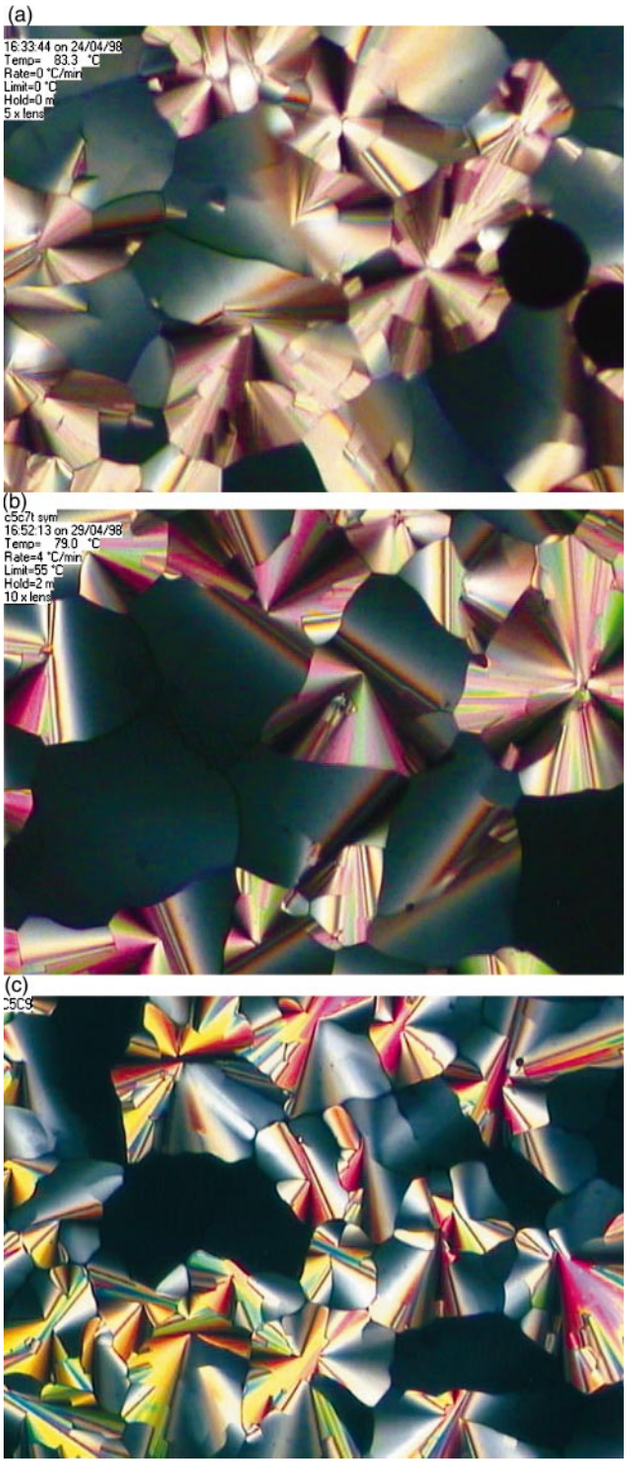

Fig. 4 Mesophase textures for (a) $\mathbf{C_5C_3}$**.sym**, (b) $\mathbf{C_5C_7}$**.sym** and (c) $\mathbf{C_5C_9}$**.sym**, viewed through crossed polarizers.

(001) peak at $\theta \approx 12.5^\circ$ corresponds to the repeat distance ($d_{intra} = d_{001}$) of the triphenylene cores along the columns. The observed values of *ca.* 3.6 Å are typical for π–π stacking.[8] The position of the broad (001) peak is temperature dependent, such that d_{intra} increases on increasing temperature. For *Series I* materials, the value of d_{intra} is 3.55 Å at the low temperature end of the mesophase, whereas close to the clearing temperature d_{intra} is *ca.* 3.65 Å (Fig. 7). In addition, the peaks become broader with increasing temperature, indicating a decrease in the degree of ordering along the columns (for example, Fig. 3a). This observation may be interpreted on the basis that the average length of the ordered domains along the column decrease as temperature is increased. Furthermore, on

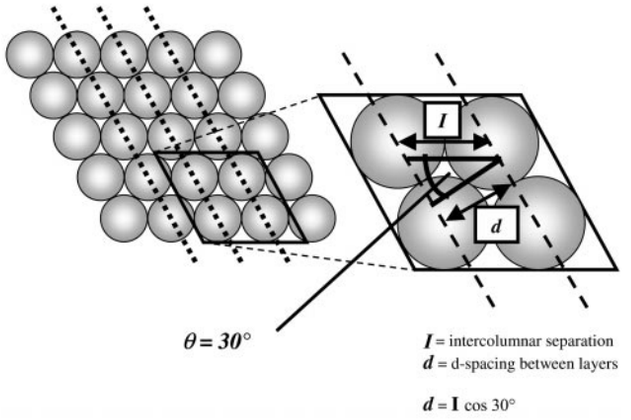

Fig. 5 Definitions of d_{100} and intercolumnar spacing for the Col_h mesophase.

increasing n, we note that the width of the (001) peak increases (Fig. 8) and exhibits an odd–even effect.

2.2.3. DSC Analysis. The phase transition temperatures were initially established from the POM studies and then measured accurately by DSC. The mesophase ranges of the *Series I* and *II* materials are shown in Fig. 9a–d, and transition enthalpies ($\Delta H_{Col–I}$) and transition entropies ($\Delta S_{Col–I}$) are shown in Fig. 10a and 10b. Table 1 details the phase transition data for *Series I* materials. Mesogenic behaviour is observed for $\mathbf{C_5C_n}$ materials with $n \geqslant 3$. This observation is interesting because $\mathbf{C_5C_3}$ is the constitutional isomer of $\mathbf{C_4C_4}$, the member of the $\mathbf{C_xC_x}$ series with the smallest value of x that forms a mesophase. Fig. 9c illustrates an increase in clearing temperature from $\mathbf{C_5C_3}$**.sym** ($T_c = 105\,^{\circ}C$) to $\mathbf{C_5C_4}$**.sym** ($T_c = 129\,^{\circ}C$). On further increasing n, the clearing temperature decreases to 122 °C ($\mathbf{C_5C_5}$) and finally to 59 °C ($\mathbf{C_5C_9}$). This decrease in clearing temperature is similar to that observed in the $\mathbf{C_xC_x}$ (for $x \geqslant 4$). $\mathbf{C_4C_4}$ exhibits the highest T_c for the $\mathbf{C_xC_x}$ series, with T_c decreasing as x increases (Fig. 9b).[27] Fig. 9b also shows that the mesophase ranges vary with n for $\mathbf{C_5C_n}$ materials. The mesophase range reaches a maximum for $\mathbf{C_5C_4}$**.sym** (74 °C) and is then depressed as n increases. Additionally, direct comparisons of constitutional isomers in the $\mathbf{C_xC_x}$ and $\mathbf{C_5C_n}$ series reveals in all cases that the $\mathbf{C_xC_x}$ compound displays a larger mesophase range and a higher clearing temperature.

On comparing the '**sym**' and '**asym**' isomers of the compounds in *Series I*, it is apparent that the molecular symmetry has little effect on the melting points and clearing temperatures, with the exception of $\mathbf{C_5C_9}$**.asym**, which exhibits lower melting and clearing temperatures. It is interesting to note that $\mathbf{C_5C_9}$**.asym** exhibits a mesophase at room temperature, which could provide the basis for potential applications under ambient conditions.

Comparison of Fig. 9b and 9c highlights the difference between the $\mathbf{C_xC_x}$ materials and the $\mathbf{C_mC_n}$**.sym** isomers of *Series I* materials. Looking at the crystal to mesophase transition (K–Col_h), for $\mathbf{C_mC_n}$**.sym** materials in the range $n = 3$–8, there is an odd–even effect in the temperature of the transition. This behaviour is not apparent in the $\mathbf{C_xC_x}$ series, and may indicate one (or both) of the following effects: (i) the crystalline packing dictates the melting to the mesophase, with more favourable packing for the 'even' (combined number of carbon atoms in the two types of alkyl chain is even) compounds and/or (ii) the mesophase interactions are more favourable for 'odd' compounds. Fig. 9c and 9d illustrate the differences in the transition temperatures between $\mathbf{C_mC_n}$**.sym** and $\mathbf{C_mC_n}$**.asym** materials. Although some differences are observed in the mesophase range and transition temperatures between the $\mathbf{C_mC_n}$**.sym** and $\mathbf{C_mC_n}$**.asym** isomers, they are not as significant as the differences between the $\mathbf{C_mC_n}$**.sym** and the

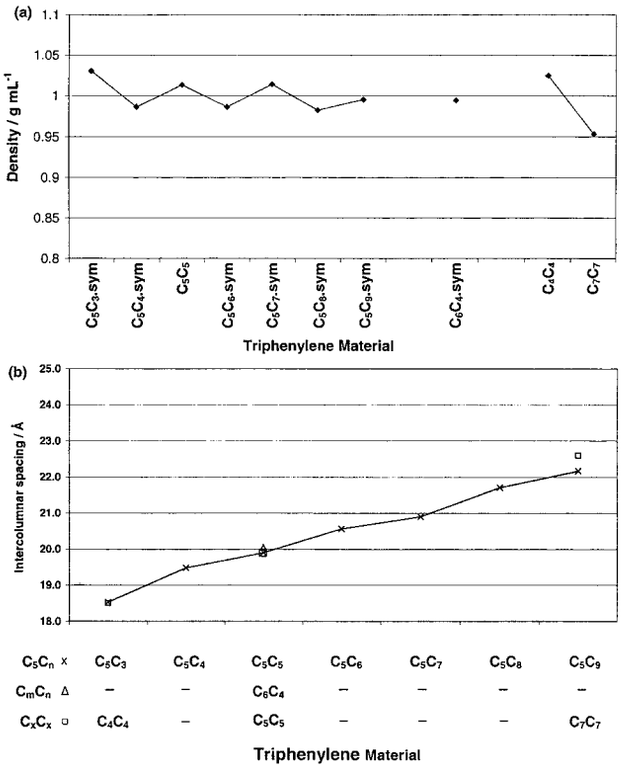

Fig. 6 (a) Calculated densities for $\mathbf{C_mC_n}$**.sym** (*Series I* and *II*) materials and $\mathbf{C_xC_x}$ materials. (b) Intercolumnar spacings for $\mathbf{C_mC_n}$**.sym** (*Series I*) materials(× ,fullline),$\mathbf{C_mC_n}$**.sym**(*SeriesII*)*materials,*$\mathbf{C_6C_4}$**.sym**(△),$\mathbf{C_xC_x}$ $\mathbf{C_xC_x}$ triphenylenes corresponding to the average chain length of the $\mathbf{C_mC_n}$**.sym** material (□).

$\mathbf{C_xC_x}$ materials. Presumably, at least at short range, the '**asym**' isomers are able to interdigitate to approximately the same extent as the '**sym**' isomers. However, this interdigitated arrangement may not be so readily propagated to long range in the '**asym**' isomers. It would appear that, due to the fluid nature of the mesophases, the short range interdigitation of the '**asym**' isomers is sufficient to obtain similar thermal properties to the '**sym**' isomers.

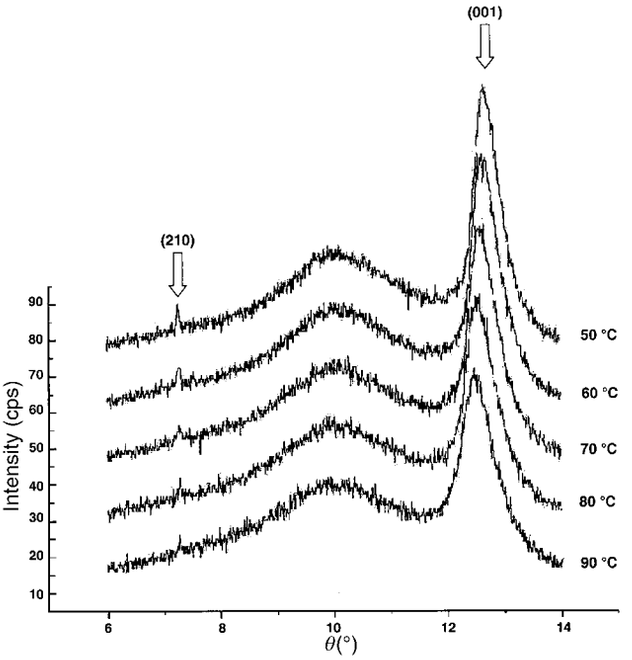

Fig. 7 The temperature dependence of the (210) and (001) reflections and d_{intra} for $\mathbf{C_5C_3}$**.sym**.

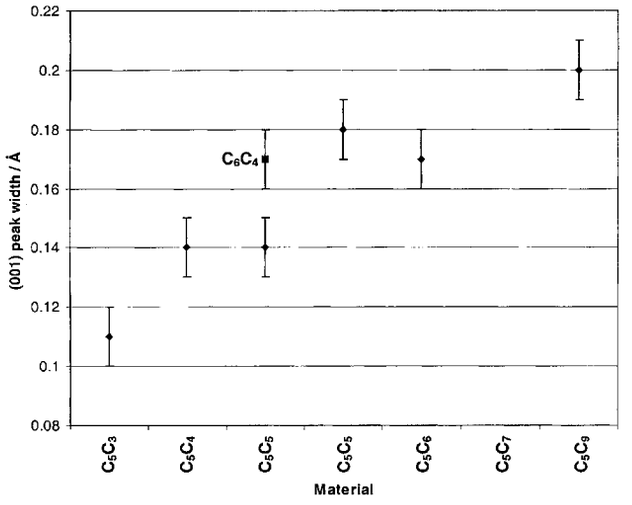

Fig. 8 Widths of (001) peak for *Series I* and *Series II* materials, measured from photographic film.

Analysis of the enthalpy and entropy data of *Series I* materials for the $Col_h \rightarrow I$ transition shows interesting patterns. As shown in Fig. 10a, $\mathbf{C}_m\mathbf{C}_n$**.sym** and $\mathbf{C}_m\mathbf{C}_n$**.asym** materials from *Series I* and *II* have similar values (~ 3 kJ mol^{-1}) of the enthalpy change for this transition. In comparison, the enthalpy change for $\mathbf{C}_x\mathbf{C}_x$ materials is higher than that of their constitutional isomers in *Series I* at short chain lengths, but is similar (converging to ~ 3 kJ mol^{-1}) at longer chain lengths. The same pattern exists for the entropy changes for the $Col_h \rightarrow I$ transition (Fig. 10b). These results suggest that, relative to the isotropic liquid, the $\mathbf{C}_m\mathbf{C}_n$ mesophases and the higher homologues of the $\mathbf{C}_x\mathbf{C}_x$ series have low enthalpic stability and a low degree of order. We suggest that the interdigitation may decrease the mesophase stability primarily through the slippage process (Fig. 3b). This process may become available to the longer chain members of the $\mathbf{C}_x\mathbf{C}_x$ series due to the fact that the amount of available 'free space' between the adjacent alkyl chains increases, and may be filled by the alkyl chains of neighbouring molecules. In Fig. 11a, the intercolumnar spacings[8,50] of $\mathbf{C}_x\mathbf{C}_x$ materials are plotted as a function of the chain length x, and shows that the relationship between intercolumnar spacing and x is not linear. In particular, as the alkyl chain length (x) increases, the increment in intercolumnar spacing per methylene group decreases (*i.e.* the gradient of the plot in Fig. 11a decreases, although still remains positive, as x increases). This observation is consistent with the fact that, as shown in Fig. 11b, there is an increase in the 'free space' between alkyl chains in a $\mathbf{C}_x\mathbf{C}_x$ molecule as x increases, with the proposal this free space becomes filled by alkyl chains of neighbouring molecules to a greater extent as x increases. Thus, the mesophase stability of $\mathbf{C}_x\mathbf{C}_x$ materials may be expected to decrease as the alkyl chain length increases.

2.3. *Series II*

2.3.1. Optical characterisation. Only two members of *Series II* exhibit mesogenic behaviour, namely $\mathbf{C_5C_5}$ and $\mathbf{C_6C_4}$**.sym**. In POM studies, both of these compounds exhibit a defect texture typical of the Col_h phase, Fig. 12a and 12b.

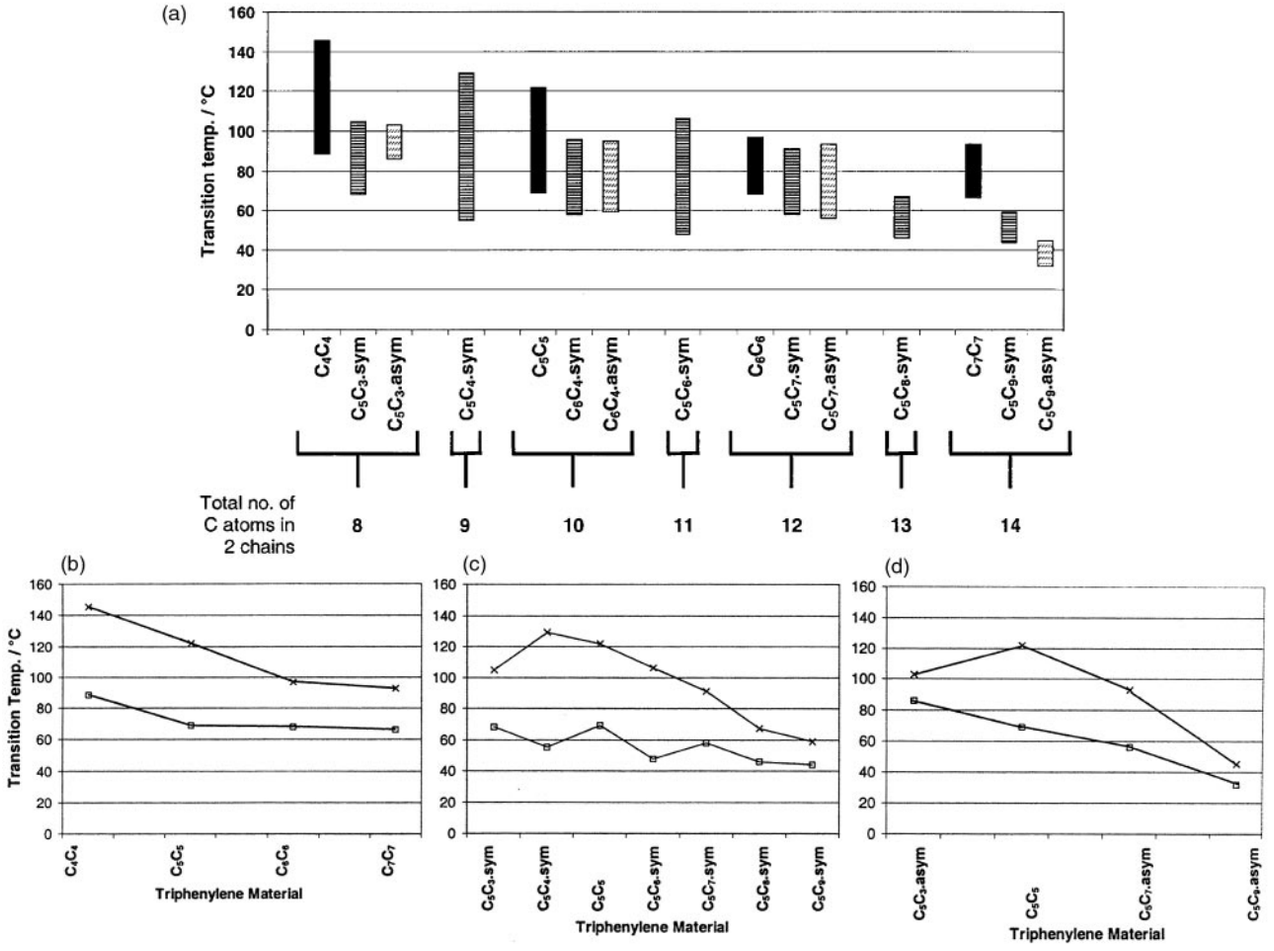

Fig. 9 (a) Mesophase ranges for *Series I* and *II* materials ('sym' and 'asym'), and their $\mathbf{C}_x\mathbf{C}_x$ constitutional isomers. (b) Phase transitions of $\mathbf{C}_x\mathbf{C}_x$ triphenylene materials. (c) Phase transitions of symmetrical isomers of *Series I* and *II* mesogenic materials. (d) Phase transitions of asymmetrical isomers of *Series I* and *II* mesogenic materials.

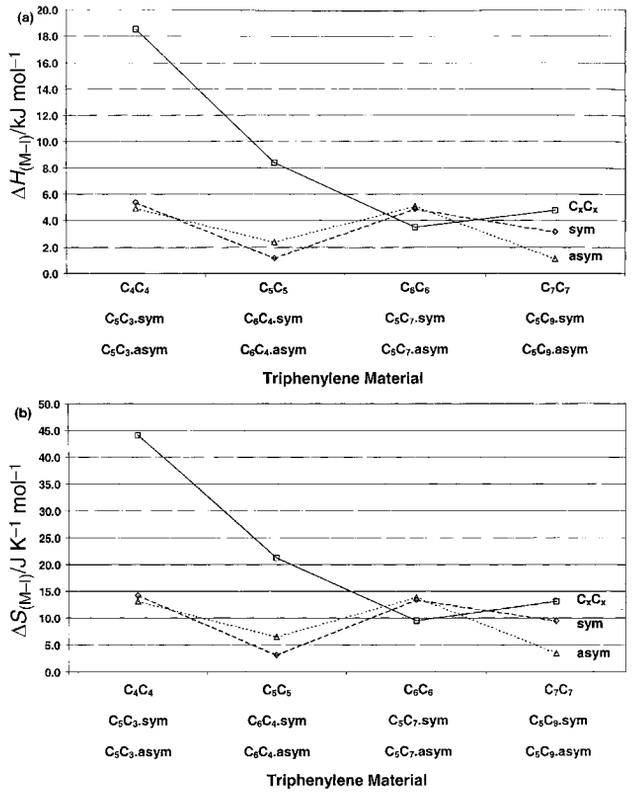

Fig. 10 (a) Phase transition enthalpy data for *Series I* and *II* materials, compared to literature values for $\mathbf{C}_x\mathbf{C}_x$ materials. (b) Phase transition entropy data for *Series I* and *II* materials, compared to literature values for $\mathbf{C}_x\mathbf{C}_x$ materials.

2.3.2. X-Ray diffraction analysis. Identification of the mesophases of *Series II* compounds by XRD also verifies that they are Col_h in nature. The intercolumnar spacing for **C_6C_4.sym**, calculated from the *d*-spacing of the (100) reflection, is 20.1 Å, which is very similar to the intercolumnar spacing for **C_5C_5** (19.9 Å), a constitutional isomer of **C_6C_4.sym**. This observation suggests that the molecules adopt a reasonably effective space filling motif, achieved by interdigitation of alkyl chains.

Table 1 Averaged thermal data for *Series I* and *Series II* materials. Transition temperatures, enthalpies and entropies were recorded by DSC on heating, at rates of 5, 10 and 20 °C min^{-1}. The heating cycles gave phase transition data which agreed to ±2%

Compound	Transition	Transition temp./°C	ΔI/kJ mol^{-1}	ΔS/J K^{-1} mol^{-1}
C_5C_1	Cr→I	142	56.03	134.03
C_5C_2	Cr→I	108	40.66	106.68
C_5C_3	Cr→Col_h	68	30.71	89.02
	Col_h→I	105	5.44	14.38
C_5C_4	Cr→Col_h	55	21.71	66.16
	Col_h→I	129	10.09	25.22
C_5C_5	Cr→Col_h	69	34.48	100.81
	Col_h→I	122	8.20	20.75
C_5C_6	Cr→Col_h	48	28.28	82.65
	Col_h→I	106	5.76	15.19
C_5C_7	Cr→Col_h	58	31.73	95.18
	Col_h→I	91	4.87	13.28
C_5C_8	Cr→Col_h	46	21.61	65.26
	Col_h→I	67	2.11[a]	6.21[a]
C_5C_9	Cr→Col_h	44	61.27	191.44
	Col_h→I	59	3.15	9.41
C_6C_4	Cr→Col_h	58	38.95	117.62
	Col_h→I	96	1.17	3.17
C_7C_3	Cr→I	66	45.17	133.19
C_8C_2	Cr→I	65	47.71	141.09

[a]Data recorded on cooling cycle at 10 °C min^{-1}.

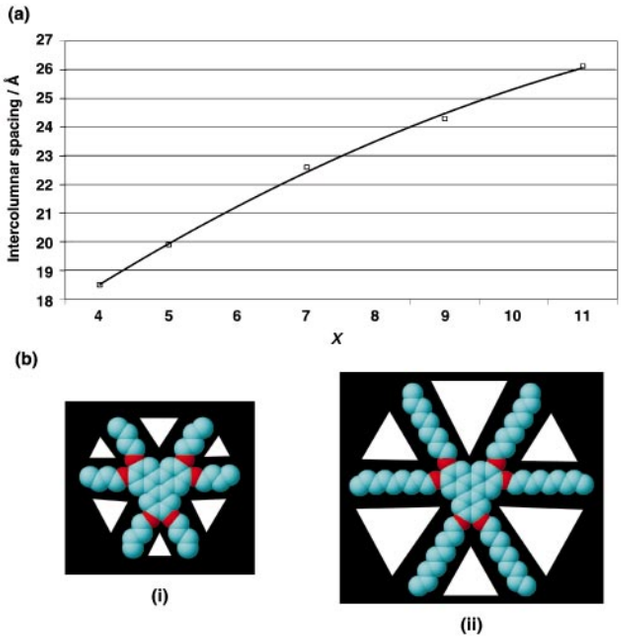

Fig. 11 (a) Intercolumnar spacing of $\mathbf{C}_x\mathbf{C}_x$ materials as a function of chain length, *x*. (b) An illustration of the increase in 'free-space' (indicated by the white regions) between alkyl chains with increasing alkyl chain length for (i) **C_4C_4** and (ii) **C_9C_9** triphenylene materials.

The intracolumnar stacking distance, determined from the *d*-spacing for the (001) peak is ~3.6 Å, with similar peak widths for **C_5C_6.sym** (IL = 1) and **C_5C_7.sym** (IL = 2), as illustrated in Fig. 8.

2.3.3. DSC Analysis. Phase transition data for *Series II* materials are shown in Table 1. Thermodynamic data are included in Fig. 10a and 10b. The mesophase range of **C_6C_4.sym** is comparable with *Series I* materials. Indeed, the mesophase range and T_c value of **C_6C_4.sym** is similar to **C_5C_7.sym**, which also has IL = 2. The fact that only **C_6C_4** and **C_5C_5** exhibit mesophases within *Series II* reflects the delicate balance between anisotropy and isotropy. Clearly, when three heptyloxy chains are present, three propyloxy chains are not sufficient to stabilise the material to the degree required to exhibit a mesophase. Indeed, perhaps the additional interaction present through interdigitation may prevent the formation of a mesophase. Enthalpy and entropy arguments are similar to those for *Series I*. Thus, the enthalpy change for **C_6C_4** is around ~3 kJ mol^{-1}, similar to that for interdigitated materials in *Series I*, with a slight difference between the symmetric and asymmetric isomers.

3. Concluding remarks

In this paper we have presented the first examples of triphenylene-based liquid crystals, which interdigitate by design. The successful synthesis of two systematic series of materials has allowed structural and thermal properties to be rationalised on the basis of the effects of varying the relative and absolute lengths of the two types of alkyl chain in the molecule. X-Ray diffraction and differential scanning calorimetry have highlighted several interesting issues, which may be interpreted on the basis of the effect and influence of interdigitation of alkyl chains. From these results, we conclude that the interdigitation leads to a decrease in mesophase stability, which may be interpreted in terms of the effects of the slippage process dominating over the rotational dynamics.

Further aspects of these materials are under investigation, including studies of dynamic properties by means of ^{2}H NMR spectroscopy of the mesophases. Photoconductivity measurements will also be made in the near future on *Series I* and *II*

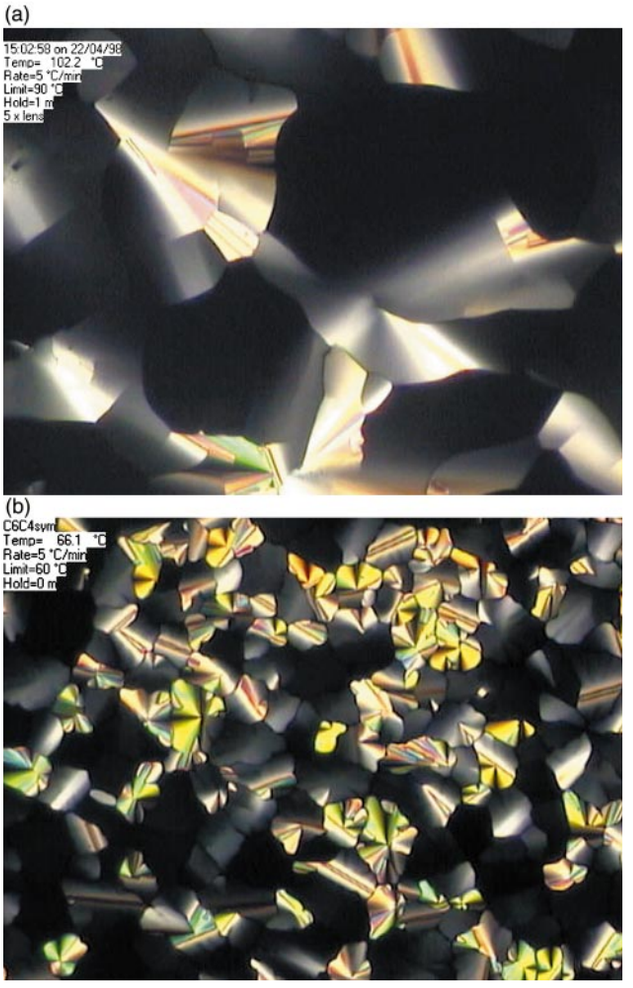

Fig. 12 Mesophase textures for (a) $\mathbf{C_5C_5}$ and (b) $\mathbf{C_6C_4}$, viewed through crossed polarizers.

materials. In addition, we are currently synthesising a third series of materials, which are constitutional isomers of $\mathbf{C_9C_9}$ (*i.e.* $\mathbf{C_{10}C_8}$, $\mathbf{C_{11}C_7}$, $\mathbf{C_{12}C_6}$ and $\mathbf{C_{13}C_5}$), analogous to *Series II*. It is anticipated that this series should generate a greater number of mesogens than *Series II*, and will contribute substantially towards progress in developing a complete understanding of the structural and thermal effects introduced by incorporating interdigitation as an organisational motif.

4. Experimental

General procedures

All chemicals were purchased from Aldrich and used without further purification. Dry CH_2Cl_2 was prepared by distillation over CaH_2 under a N_2 atmosphere. Thin Layer Chromatography (TLC) was performed on aluminium sheets coated with silica gel 60 F_{254} (Merck 5554, 230–400 mesh). Initial inspection of TLC plates was by use of UV light, and subsequent development by iodine vapour or 5% $CeSO_4$ solution in EtOH, followed by heating. Column chromatography was carried out using silica gel 60 F_{254} (Merck 9385, 230–400 mesh).

^{1}H NMR spectra were recorded on a Bruker AC300 (300 MHz) spectrometer. ^{13}C NMR were recorded on a Bruker AC300 (75.5 MHz) spectrometer using the pendant pulse sequence. All chemical shifts are quoted in ppm on the δ scale, with all coupling constants expressed in hertz (Hz), using residual solvent as the internal standard.

Mass spectra were obtained using Electron Impact Mass Spectrometry (EIMS), from a VG ProSpec mass spectrometer, or Liquid Secondary Ion Mass Spectra (LSIMS), from a VG ZabSpec mass spectrometer, equipped with a caesium ion source.

Optical microscopy experiments were carried out using a Boetius hot stage microscope. Photographs were taken on a Nikon Optiphot 2 polarizing microscope, equipped with a Mettler FP 82 HT heating stage and a camera. In addition, video capture images were recorded on an Olympus BX40 optical microscope, with crossed polarizers, equipped with a Linkam LT350 hot stage.

Differential Scanning Calorimetry (DSC) results were recorded on a Perkin-Elmer 7 Series and a Perkin-Elmer Pyris thermal analysis system. All samples were subjected to 2 heating and cooling cycles, heating to 150–180 °C (at least 30 °C above a sample's T_C) and cooled to −30 °C, at a rate of 10 K min^{-1}.

Mesophase X-ray diffraction was carried out on a Huber Guinier Pulverkammer 621 variable temperature diffractometer, using Cu Kα radiation. Both photographic and diffractometric measurements were used.

1,2-Bis(pentyloxy)benzene, 1

To a stirred solution of catechol (25.0 g, 0.227 mol) in MeCN (500 mL) was added K_2CO_3 (160.0 g, 1.140 mol). The slurry was heated under reflux for 30 minutes under a N_2 atmosphere. A solution of 1-bromopentane (76.0 g, 0.500 mol) in MeCN (100 mL) was added dropwise to the slurry, maintaining the reflux and stirring. The mixture was heated under reflux for 20 hours. The reaction was cooled to room temperature and filtered. The inorganic residue was washed with CH_2Cl_2 (2×50 mL). The filtrate was concentrated *in vacuo* and dissolved in CH_2Cl_2 (100 mL). The organic layer was washed with NaOH solution (0.5 M, 50 mL), followed by water (2×50 mL). The organic layer was dried ($MgSO_4$). The drying agent was removed by filtration, the inorganic residue washed with CH_2Cl_2 (2×25 mL) and concentrated *in vacuo*, yielding a light brown oil, **2** (48 g, 83%). *m*/*z* (EI) 250 $[M]^+$; δ_H (300 MHz, $CDCl_3$) 6.89 (4H, s, Ar-*H*), 3.99 (4H, t, $J=6.6$, OCH_2), 1.82 (4H, quintet, $J=7.4$, CH_2), 1.32–1.52 (8H, m, CH_2), 0.92 (6H, t, $J=7.2$, CH_3); δ_C (75 MHz, $CDCl_3$) 149.2, 121.0, 114.0, 69.2, 29.1, 28.3, 22.5, 14.1.

2,3,6,7,10,11-Hexakis(pentyloxy)triphenylene, $\mathbf{C_5C_5}$

A solution of **1** (5.30 g, 21 mmol) in dry CH_2Cl_2 (40 mL) was degassed with N_2 for 15 minutes. The reaction flask was covered in aluminium foil and the solution stirred under a N_2 atmosphere, with a $CaCl_2$ drying arm attached. $MoCl_5$ (6.37 g, 23 mmol) was added to the solution quickly but with care. The reaction was stirred at room temperature for 20–30 minutes and was carefully monitored by TLC [eluent: petroleum ether (bp 60–80 °C)–acetone (5 : 1)], until all of **2** had reacted. The reaction vessel was placed in an ice bath and the reaction quenched with ice-cold MeOH (75 mL). The mixture was stirred for 60 minutes at 0 °C, precipitating a white solid. The reaction mixture was filtered and the residue washed with ice-cold MeOH (2×15 mL). The precipitate was purified by 2 recrystallisations from MeOH, yielding a white, flaky solid of $\mathbf{C_5C_5}$ (3.35 g, 64%). *m*/*z* (EI) 745 $[M]^+$; δ_H (300 MHz, $CDCl_3$) 7.85 (6H, s, Ar-*H*), 4.25 (12H, t, $J=6.6$, OCH_2), 1.92–1.99 (12H, m, CH_2), 1.42–1.67 (24H, m, CH_2), 0.99 (18H, t, $J=7.4$, CH_3); δ_C (75 MHz, $CDCl_3$) 148.9, 123.6, 107.2, 69.7, 28.4, 22.6, 14.2 {Found: C 77.31, H 9.72. Calc. for $C_{48}H_{72}O_6$: C 77.38 H 9.74}.

2,6,10-Tris(pentyloxy)-3,7,11-trihydroxytriphenylene, $\mathbf{C_5C_0}$.sym; 2,7,10-tris(pentyloxy)-3,6,11-trihydroxytriphenylene $\mathbf{C_5C_0}$.asym

A solution of $\mathbf{C_5C_5}$ (2.23 g, 3.00 mmol) in dry CH_2Cl_2 (25 mL) was degassed with N_2 for 15 minutes. A solution of 9-Br-BBN

in CH_2Cl_2 (1.0 M, 13.5 mL, 13.5 mmol) was added dropwise to the solution over 60 minutes under an atmosphere of N_2, whilst the solution was stirred at 0 °C. The reaction mixture was stirred for a further 8 hours at 0 °C. The reaction vessel was then transferred to the freezer for a further 30 hours. The reaction was carefully quenched with 2-aminoethanol (25 mL). The mixture was diluted with water (25 mL) and the products extracted into CH_2Cl_2 (2 × 25 mL). The organic layer was dried ($MgSO_4$). The drying agent was removed by filtration and the filtrate was concentrated *in vacuo*. The two constitutional isomeric products were isolated from the crude mixture using silica gel chromatography [eluent:CH_2Cl_2–MeOH (100 : 1)].

C_5C_0sym. (0.67 g, 42%); *m/z* (EI) 534 $[M]^+$; δ_H (300 MHz, $CDCl_3$) 7.91 (3H, s, Ar-*H*), 7.78 (3H, s, Ar-*H*), 5.91 (3H, s, O*H*), 4.24 (6H, t, $J=6.6$, OCH_2), 1.89–1.98 (6H, quintet, $J=7.1$, CH_2), 1.38–1.62 (12H, br m, CH_2), 0.98 (9H, t, $J=7.2$, CH_3); δ_C (75 MHz, $CDCl_3$) 145.7, 145.2, 123.8, 122.8, 106.9, 104.5, 69.0, 29.0, 28.2, 22.6, 14.1.

C_5C_0asym. (0.48 g, 30%); δ_H (300 MHz, $CDCl_3$); 7.70–7.95 (6H, m, Ar-*H*), 5.87 (3H, t, $J=5.46$, O*H*), 4.25 (6H, m, OCH_2), 1.76–2.00 (6H, br m, CH_2), 1.38–1.70 (12H, br m, CH_2), 0.97 (3H, dt, CH_3); δ_C (75 MHz, $CDCl_3$) 145.3, 122.9, 107.7, 107.4, 107.2, 104.3, 104.2, 104.0, 69.1, 56.4, 28.3, 22.6, 14.1.

2,6,10-Tris(pentyloxy)-3,7,11-tris(alkyloxy)triphenylene, C_5C_n

Typical quantities for this homologous set of reactions are shown in Table S1 in Supplementary Information.

K_2CO_3 was added to a solution of **C_5C_0.sym** in MeCN. The slurry was heated under reflux for 30 minutes under a N_2 atmosphere. A solution of (R^1–Hal) in MeCN was added dropwise to the slurry, maintaining the reflux and stirring. The mixture was heated under reflux for 20 hours. The reaction was cooled to room temperature and filtered; the residue was washed with CH_2Cl_2 (2 × 25 mL). The filtrate was concentrated *in vacuo*. The crude, white solid was subjected to two recrystallisations from MeOH or EtOH, yielding white/yellow solids of the triphenylene derivatives. Spectroscopic data are shown in Table S2 in Supplementary Information.

2,6,10-Tris(hexyloxy)-3,7,11-tris(butyloxy)triphenylene, C_6C_4

The synthesis of 1,2-bis(hexyloxy)benzene, **2**, was carried out in a similar fashion to 1,2-bis(pentyloxy)benzene, **1**, replacing 1-bromopentane with 1-bromohexane yielding a dark brown oil, **2** (9.1 g, 72%). The synthesis of hexakis(hexyloxy)triphenylene, **C_6C_6**, was carried out in a similar fashion to hexakis(pentyloxy)triphenylene, **C_5C_5**, using **2** in place of **1**, yielding a flaky, white solid, **C_6C_6** (0.89 g, 43%). The synthesis of 2,6,10-trihydroxy-3,7,11-tris(hexyloxy)triphenylene, **C_6C_0.sym**, was carried out in a similar fashion to 2,6,10-trihydroxy-3,7,11-tris(pentyloxy)triphenylene, **C_5C_0.sym**, using **C_6C_6** in place of **C_5C_5**, yielding a fine, white powder, **C_6C_0.sym**. (0.21 g, 35%); δ_H (300 MHz, $CDCl_3$) 7.92 (3H, s, Ar-*H*), 7.79 (3H, s, Ar-*H*), 4.25 (6H, t, $J=6.6$, OCH_2), 1.93 (6H, quintet, $J=7.1$, CH_2), 1.35–1.56 (18H, br m, CH_2), 0.94 (9H, t, $J=7.0$, CH_3). To a solution of **C_6C_0.sym** (0.20 g, 0.35 mmol) in CH_3CN (10 mL) was added K_2CO_3 (0.41 g, 2.97 mmol). The slurry was heated under reflux for 30 minutes under a N_2 atmosphere. 1-bromobutane (0.21 g, 1.48 mmol) was added dropwise to the slurry, maintaining the reflux and stirring. The mixture was heated under reflux for 20 hours. The reaction was cooled to room temperature and filtered; the residue was washed with CH_2Cl_2 (2 × 10 mL). The filtrate was concentrated *in vacuo*. The crude, white solid was subjected to two recrystallisations from EtOH, yielding a pale yellow solid, **C_6C_4** (0.23 g, 89%). *m/z* (LSIMS) 745 $[M+H]^+$; δ_H (300 MHz, $CDCl_3$) 7.83 (6H, s, Ar-*H*), 4.23 (6H, t, $J=6.4$, OCH_2), 4.22 (6H, t, $J=6.6$, OCH_2), 1.88–1.98 (12H, br m, CH_2), 1.03 (9H, t, $J=7.4$, CH_3), 0.93 (9H, t, $J=7.0$, CH_3); δ_C (75 MHz, $CDCl_3$) 149.0, 123.6, 107.3, 69.7, 69.4, 25.9, 22.7, 19.4, 14.0 {Found: C 77.74, H 9.49. Calc. for C_{48} H_{72} O_6: C 77.42, H 9.68}.

2,6,10-Tris(heptyloxy)-3,7,11-tris(propyloxy)triphenylene, C_7C_3

The synthesis of 1,2-bis(heptyloxy)benzene, **3**, was carried out in a similar fashion to 1,2-bis(pentyloxy)benzene, **1**, replacing 1-bromopentane with 1-bromoheptane, yielding a brown oil, **3** (4.8 g, 68%). The synthesis of hexakis(heptyloxy)triphenylene, **C_7C_7**, was carried out in a similar fashion to hexakis(pentyloxy)triphenylene, **C_5C_5**, using **3** in place of **1**, yielding a flaky, white solid, **C_7C_7** (0.91 g, 30%). The synthesis of 2,6,10-trihydroxy-3,7,11-tris(heptyloxy)triphenylene, **C_7C_0.sym**, was carried out in a similar fashion to 2,6,10-trihydroxy-3,7,11-tris(pentyloxy)triphenylene, **C_5C_0.sym**, using **C_7C_7** in place of **C_5C_5**, yielding a fine, white powder, **C_7C_0.sym** (0.08 g, 30%); δ_H (300 MHz, $CDCl_3$) 7.91 (3H, s, Ar-*H*), 7.79 (3H, s, Ar-*H*), 4.25 (6H, t, $J=4.3$, OCH_2), 1.93 (6H, quintet, $J=7.0$, CH_2), 1.34–1.59 (24H, br m, CH_2), 0.91 (9H, t, $J=6.8$, CH_3). To a solution of **C_7C_0.sym** (0.07 g, 0.11 mmol) in CH_3CN (20 mL) was added K_2CO_3 (0.13 g, 0.90 mmol). The slurry was heated under reflux for 30 minutes under a N_2 atmosphere. 1-bromopropane (0.07 g, 0.57 mmol) was added dropwise to the slurry, maintaining the reflux and stirring. The mixture was heated under reflux for 20 hours. The reaction was cooled to room temperature and filtered; the residue was washed with CH_2Cl_2 (2 × 10 mL). The filtrate was concentrated *in vacuo*. The crude, white solid was subjected to two recrystallisations from EtOH, yielding a pale yellow solid, **C_7C_3** (0.06 g, 74%). *m/z* (LSIMS) 745 $[M+H]^+$; δ_H (300 MHz, $CDCl_3$) 7.83 (6H, s, Ar-*H*), 4.23 (6H, t, $J=6.6$, OCH_2), 4.19 (6H, t, $J=6.6$, OCH_2), 1.89–2.03 (12H, br m, CH_2), 1.33–1.61 (24H, br m, CH_2), 1.14 (9H, t, $J=7.4$, CH_3), 0.90 (9H, t, $J=6.8$, CH_3); δ_C (75 MHz, $CDCl_3$) 149.0, 123.6, 107.4, 71.2, 69.7, 31.9, 29.2, 26.2, 14.2, 10.7 {Found: C 77.62, H 9.71. Calc. for C_{48} H_{72} O_6: C 77.42, H 9.68}.

2,6,10-Tris(octyloxy)-3,7,11-tris(ethyloxy)triphenylene, C_8C_2

The synthesis of 1,2-bis(octyloxy)benzene, **4**, was carried out in a similar fashion to 1,2-bis(pentyloxy)benzene, **1**, replacing 1-bromopentane with 1-bromooctane, yielding a brown oil, **4** (8.8 g, 58%). δ_H (300 MHz, $CDCl_3$) 6.88 (4H, s, Ar-*H*), 3.99 (4H, t, $J=6.8$, OCH_2), 1.81 (4H, quintet, $J=7.0$, CH_2), 1.28–1.51 (20H, br m, CH_2), 0.88 (6H, t, $J=6.8$, CH_3). The synthesis of hexakis(heptyloxy)triphenylene, **C_8C_8**, was carried out in a similar fashion to hexakis(pentyloxy)triphenylene, **C_5C_5**, using **4** in place of **1**, yielding a flaky, white solid, **C_8C_8** (1.07 g, 49%). The synthesis of 2,6,10-trihydroxy-3,7,11-tris(octyloxy)triphenylene, **C_8C_0.sym**, was carried out in a similar fashion to 2,6,10-trihydroxy-3,7,11-tris(pentyloxy)triphenylene, **C_5C_0.sym**, using **C_8C_8** in place of **C_5C_5**, yielding a fine, white powder, **C_8C_0.sym** (0.18 g, 27%); δ_H (300 MHz, $CDCl_3$) 7.91 (3H, s, Ar-*H*), 7.78 (3H, s, Ar-*H*), 4.24 (6H, t, $J=6.6$, OCH_2), 1.93 (6H, quintet, $J=7.0$, CH_2), 1.25–1.57 (30H, br m, CH_2), 0.90 (9H, t, $J=6.8$, CH_3). To a solution of **C_8C_0.sym** (0.15 g, 0.22 mmol) in CH_3CN (20 mL) was added K_2CO_3 (0.30 g, 2.17 mmol). The slurry was heated under reflux for 30 minutes under a N_2 atmosphere. 1-bromoethane (0.18 g, 1.63 mmol) was added dropwise to the slurry, maintaining the reflux and stirring. The mixture was heated under reflux for 20 hours. The reaction was cooled to room temperature and filtered; the residue was washed with CH_2Cl_2 (2 × 10 mL). The filtrate was concentrated *in vacuo*. The crude, white solid was subjected to two recrystallisations from EtOH, yielding a pale yellow solid, **C_8C_2** (0.10 g, 58%). *m/z* (LSIMS) 745 $[M+H]^+$; δ_H (300 MHz, $CDCl_3$) 7.84 (3H, s, Ar-*H*), 7.83 (3H, s, Ar-*H*), 4.31 (6H, q, $J=7.0$, OCH_2), 4.23 (6H, t, $J=6.6$, OCH_2), 1.90–1.99 (6H, q,

$J = 7.2$, CH_2), 1.25–1.58 (39H, br m, CH_2, CH_3), 0.89 (9H, t, $J = 6.8$, CH_3); δ_C (75 MHz, $CDCl_3$) 149.0, 148.7, 123.7, 123.5, 115.5, 107.5, 107.0, 70.9, 70.8, 69.8, 69.6, 65.3, 31.9, 29.5, 29.4, 26.2, 22.7, 15.9, 14.2 {Found: C 77.55, H 9.83. Calc. for C_{48} H_{72} O_6: C 77.42, H 9.68}.

Acknowledgements

We are grateful to EPSRC, HEFCE, Perkin Elmer and NATO for financial support.

References

1 S. Chandrasekhar, B. K. Sadashiva and K. A. Suresh, *Pramana*, 1977, **9**, 471.
2 J. Billare, J. C. Dubois, N. H. Tinh and A. Zann, *Nouv. J. Chim.*, 1978, **2**, 535.
3 C. Destrade, J. Malthête and M. C. Mondon, *J. Phys. (Paris)*, 1979, **40**, C3–17.
4 R. J. M. Nolte, C. F. van Nostrum, S. J. Picken and A.-J. Schouten, *J. Am. Chem. Soc.*, 1995, **117**, 9957.
5 H. Bock and W. Helfrich, *Liq. Cryst.*, 1992, **12**, 697.
6 V. Minter and T. J. Philips, *Liq. Cryst.*, 1996, **20**, 243.
7 J. W. Goodby, P. Hindmarsh, M. Hird and M. J. Watson, *J. Mater. Chem.*, 1995, **5**, 2111.
8 H. Bengs, F. Closs, T. Frey, D. Funhoff, H. Ringsdorf and K. Siemensmeyer, *Liq. Cryst.*, 1993, **15**, 565.
9 J. D. Brand, A. van de Craats, Y. Geerts, K. Müllen and J. M. Warman, *Adv. Mater.*, 1998, **10**, 36.
10 C. K. Lai, Y.-S. Pang and C.-H. Tsai, *J. Mater. Chem.*, 1998, **8**, 1355.
11 M.-G. Choi, S. H. Kang, H. Kim, K. Kim, S. J. Kim, K.-M. Park and W.-C. Zin, *Chem. Mater.*, 1998, **10**, 1889.
12 P. Espinet, M. C. Lequerica and J. M. Martin-Alverez, *Chem. Eur. J.*, 1999, **5**, 1982.
13 C. Destrade, H. Gasparoux, F. Hardouin, A. M. Levelut and N. H. Tinh, *J. Phys. (Paris)*, 1981, **42**, 147.
14 C. Destrade, A. M. Levelut, J. Malthete, L. Mamlock and N. H. Tinh, *J. Phys. Lett.*, 1982, **43**, L-641.
15 F. Closs, T. Frey, D. Funhoff and K. Siemensmeyer, *Liq. Cryst.*, 1993, **14**, 629.
16 M. G. Carter, in *Electronic Materials*, eds. L. S. Miller and J. B. Mullin, Plenum Press, New York, 1991.
17 G. Castro and J. F. Hornig, *J. Chem. Phys.*, 1965, **42**, 1459.
18 R. H. Batt, C. L. Braun and J. F. Hornig, *J. Chem. Phys.*, 1968, **49**, 1967.
19 P. J. Bounds and W. Siebrand, *Chem. Phys.*, 1980, **75**, 414.
20 H. Bässler, G. Peter, L. Sebastian and G. Weiser, *Chem. Phys.*, 1983, **75**, 103.
21 R. M. Schaffert, *IBM J. Res. Dev.*, 1971, **15**, 71.
22 *Handbook of Liquid Crystals*, eds. D. Demus, J. Goodby, G. W. Gray, H.-W. Speiss and V. Vill, Wiley-VCH, Weinheim, 1998.
23 D. Adam, F. Closs, T. Frey, D. Funhoff, D. Haarer, H. Ringsdorf, P. Schuhmacher and K. Siemensmeyer, *Phys. Rev. Lett.*, 1993, **70**, 457.
24 D. Adam, K.-H. Etzbach, D. Haarer, L. Haüßling, H. Ringsdorf, P. Schuhmacher, J. Simmerer and K. Siemensmeyer, *Nature*, 1994, **371**, 141.
25 M. R. Bryce, *Chem. Soc. Rev.*, 1991, **20**, 355.
26 J. B. Torrence, *Acc. Chem. Res.*, 1979, **12**, 79.
27 F. Wudl, *Acc. Chem. Res.*, 1984, **17**, 227.
28 D. Adam, D. Haarer, M. P. de Haas, P. Schuhmacher, J. Simmerer, A. M. van de Craats and J. M. Warman, *Adv. Mater.*, 1996, **8**, 823.
29 P. Carroll, P. A. Heiney, S. H. J. Idziak, J. P. McCauley and A. B. Smith III, *Mol. Cryst. Liq. Cryst.*, 1993, **237**, 271.
30 N. Boden, R. J. Bushby and A. N. Cammidge, *J. Am. Chem. Soc.*, 1995, **117**, 924.
31 B. Hüser, W. Kranig, W. Kreuder, H. Ringsdorf, H. W. Spiess and H. Zimmermann, *Adv. Mater.*, 1990, **2**, 36.
32 M. M. Green, H. Ringsdorf, J. Wagner and R. Wüstefeld, *Angew. Chem., Int. Ed. Engl.*, 1990, **29**, 1478.
33 M. Erbert, H. Ringsdorf, J. H. Wendorff, R. Wüstefeld and E. Zerta, *Angew. Chem., Int. Ed. Engl.*, 1989, **28**, 914.
34 N. Boden, R. J. Bushby, A. N. Cammidge, A. El-Mansoury, P. S. Martin and Z. Lu, *J. Mater. Chem.*, 1999, **9**, 1391.
35 S. Kumar, M. Manickam, J. A. Preece and N. Spencer, *Liq. Cryst.*, 2000, **5**, 703.
36 D. Blunk, A. Eckert and K. Praefcke, *Liq. Cryst.*, 1997, **22**, 113.
37 S. Kumar and M. Manickam, *Mol. Cryst. Liq. Cryst.*, 1998, **309**, 291.
38 N. Boden, R. J. Bushby and A. N. Cammidge, *Mol. Cryst. Liq. Cryst.*, 1995, **260**, 307.
39 P. R. Ashton, G. Hadziiannou, J. A. Preece and E. van der Vegte, *Langmuir*, 2000, **16**, 3249.
40 S. J. Cross, J. W. Goodby, A. W. Hall, M. Hird, S. M. Kelly, K. J. Toyne and C. Wu, *Liq. Cryst.*, 1998, **25**, 1.
41 P. Henderson, H. Ringsdorf and P. Schuhmacher, *Liq. Cryst.*, 1995, **18**, 191.
42 N. Boden, R. J. Bushby and A. N. Cammidge, *J. Chem. Soc., Chem. Commun.*, 1994, 465.
43 J. W. Goodby, M. Hird, K. J. Toyne and T. Watson, *J. Chem. Soc., Chem. Commun.*, 1994, 1701.
44 M. C. Bernaud, C. Destrade, G. Sigaud and N. H. Tinh, *Mol. Cryst. Liq. Cryst.*, 1981, **65**, 307.
45 M. T. Allen, S. Diele, K. D. M. Harris, T. Hegmann, B. M. Kariuki, D. Lose, J. A. Preece and C. Tschierske, *Liq. Cryst.*, 2000, **27**, 689.
46 N. Boden, R. C. Borner, R. J. Bushby, A. N. Cammidge and M. V. Jesudason, *Liq. Cryst.*, 1993, **15**, 851.
47 S. Kumar and M. Manickam, *Chem. Commun.*, 1997, 1615.
48 F. Closs, L. Häußling, P. Henderson, H. Ringsdorf and P. Schuhmacher, *J. Chem. Soc., Perkin Trans. 1*, 1995, 829.
49 S. Kumar and M. Manickam, *Synthesis*, 1998, 1119.
50 E. O. Arikainen, N. Boden, R. J. Bushby, J. Clements, B. Movaghar and A. Wood, *J. Mater. Chem.*, 1995, **5**, 2161.
51 D. Adam, K.-H. Etzbach, B. Glüsen, D. Haarer, A. Kettner, W. Paulus, H. Ringsdorf, P. Schuhmacher, K. Siemensmeyer, J. Simmerer and J. H. Wendorff, *Adv. Mater.*, 1996, **8**, 815.